BIOCHEMISTRY
including biophysical chemistry & molecular biology

ARTICLE

pubs.acs.org/biochemistry

Macromolecular Crowding Extended to a Heptameric System: The Co-chaperonin Protein 10

Ximena Aguilar, Christoph F. Weise, Tobias Sparrman, Magnus Wolf-Watz, and Pernilla Wittung-Stafshede*

Department of Chemistry, Chemical Biological Center, Umeå University, 901 87 Umeå, Sweden

Supporting Information

ABSTRACT: Experiments on monomeric proteins have shown that macromolecular crowding can stabilize toward heat perturbation and also modulate native-state structure. To assess the effects of macromolecular crowding on unfolding of an *oligomeric* protein, we here tested the effects of the synthetic crowding agent Ficoll 70 on human cpn10 (GroES in *E. coli*), a heptameric protein consisting of seven identical β-barrel subunits assembling into a ring. Using far-UV circular dichroism (CD), tyrosine fluorescence, nuclear magnetic resonance (NMR), and cross-linking experiments, we investigated thermal and chemical stability, as well as the heptamer−monomer dissociation constant, without and with crowding agent. We find that crowding shifts the heptamer−monomer equilibrium constant in the direction of the heptamer. The cpn10 heptamer is both thermally and thermodynamically stabilized in 300 mg/mL Ficoll 70 as compared to regular buffer conditions. Kinetic unfolding experiments show that the increased stability in crowded conditions, in part, is explained by slower unfolding rates. A thermodynamic cycle reveals that in presence of 300 mg/mL Ficoll the thermodynamic stability of each cpn10 monomer increases by over 30%, whereas the interfaces are stabilized by less than 10%. We also introduce a new approach to analyze the spectroscopic data that makes use of multiple wavelengths: this provides robust error estimates of thermodynamic parameters.

It is most often assumed that protein biophysical and structural properties observed in dilute buffer solutions *in vitro* also represent the *in vivo* scenario. However, the intracellular environment is highly crowded due to the presence of large amounts of soluble and insoluble biomolecules, including proteins, nucleic acids, ribosomes, and carbohydrates. It has been estimated that the concentration of macromolecules in the cytoplasm ranges from 80 to 400 mg/mL.[1] Macromolecules collectively occupy between 10 and 40% of the total volume in physiological fluids.[2] The term macromolecular crowding[3] implies the nonspecific influence of steric repulsions on specific reactions that occur in highly volume-occupied media. Because of excluded volume effects,[4] any reaction that increases the available volume will be favored by macromolecular crowding.[5] It is proposed that crowding provides a stabilizing effect to the folded state of proteins indirectly due to compaction of the more extended and malleable denatured states.[6,7]

As a result of recent advances in computational methods and resources, investigations of confinement and macromolecular crowding effects on protein conformational changes,[8,9] folding,[10,11] thermodynamics and kinetics of protein folding under confinement,[12] association,[13,14] and dynamics[15] have deepened our understanding of biopolymer dynamics under cell-like conditions. Macromolecular crowding in solution can be mimicked experimentally by adding high concentrations of inert synthetic or natural macromolecules, termed crowding agents, to the systems *in vitro*. Whereas theoretical simulations have focused on small proteins or peptides,[7] experimental crowding studies in solution have mostly involved large, complex proteins and often extreme solvent conditions. A few studies have also focused on the ability of crowding agents to induce conformational changes in unfolded states of proteins.[16,17] Recently, it has been suggested that the dominant factors affecting protein behavior *in vivo* are a combination of excluded volume effects and weak attractive forces (such as hydrodynamic interactions and electrostatics).[18−22]

We recently combined *in vitro* spectroscopic experiments and computer simulations to reveal effects of macromolecular crowding on α/β *Desulfovibrio desulfuricans* apoflavodoxin (148 residues), α-helical VlsE (327 residues), and cytochrome *c* (104 residues) at neutral pH. Apoflavodoxin and VlsE (but not cytochrome *c* which is smaller and more stable) become more structured in their folded states in response to crowding: VlsE, being aspherical, changed folded-state shape in crowded conditions.[23−25] In agreement with predictions based on the excluded volume interactions exerted by crowders, all proteins were thermally stabilized by the presence of crowding agents.

Received: February 10, 2011
Revised: March 1, 2011
Published: March 04, 2011

Figure 1. Structure of human cpn10 heptamer *hm*cpn10.[47] Flexible loops are not included in the model (each monomer has a different color). One interface is circled in blue.

To probe the effects of macromolecular crowding on a homo-oligomeric protein, we here study the human mitochondrial cochaperonin protein 10 (cpn10). Cpn10 (GroES in *E. coli*) is a homoheptameric ring-shaped protein[26−29] that normally functions as the cap to cpn60 (GroEL in *E. coli*). In the cavity inside the cpn60 ring, closed by the cpn10 ring, substrate folding is facilitated in an ATP-dependent manner.[30] In addition to the chaperonin activity, human mitochondrial cpn10 is identical to an immunosuppressive growth factor found in maternal serum,[31] and it is overexpressed during carcinogenesis[32] and in several protein-misfolding diseases.[33] Both structure and function of cpn10 appear conserved throughout nature.[26−29,34−38] In all known cases, each cpn10 subunit adopts an irregular β-barrel topology in the folded, ring-shaped heptamer (Figure 1). The dominant interaction between the subunits is an antiparallel pairing of the first β-strand in one subunit and the final β-strand in the other subunit.[34] Biophysical work on cpn10 proteins[39−44] has shown that isolated cpn10 monomers can fold but have low stability. For human and *E. coli* cpn10 species, more than three-fourths of the overall heptamer stability is governed by the interprotein interactions.[41,45]

We report that macromolecular crowding stabilizes the cpn10 heptamer toward both chemical and thermal perturbations. This arises mostly due to increased stability of each monomer; the energetic effect on interprotein interactions is small. The increased heptamer stability in Ficoll 70 is in part explained by slower unfolding kinetics. We introduce a new approach to analyze equilibrium spectroscopic data that involves analysis of multiple wavelengths.

MATERIALS AND METHODS

Protein Preparation. The expression and purification of human cpn10 were carried out as previously described[46,47] with the following minor modifications. A final concentration of 1 mM isopropyl-β-D-thiogalactopyranoside (Fermentas) was used for the overexpression with an induction time of 4 h before harvesting. Cells were disrupted by sonication using a digital sonifier (Branson). The ammonium sulfate precipitation of the supernatant was omitted. The supernatant was degassed and filtered through 0.22 μm sterile filter membrane (Millipore) before being loaded into a DEAE anion exchange column. Protein concentrations are reported per monomer units and were determined from $\varepsilon_{278} = 4200\ M^{-1}\ cm^{-1}$. A 1 L cell culture gives ~100 mg of pure protein.

Table 1. Diffusion Coefficients for cpn10 and S16[64] (Monomeric Protein, 104 Residues Long) as a Function of Denaturants (Unfolding the Proteins)[a]

	Cpn10 ($\times 10^{11}$ m^2/s)	Cpn10 $\times\ \eta_{rel}$ ($\times 10^{11}$ m^2/s)
buffer	6.2	6.2
5 M urea	6.4	8.3
2 M GuHCl	8.8	9.6
	S16	S16 $\times\ \eta_{rel}$
buffer	10.1	10.1
6 M urea	5.8	8.1
3 M GuHCl	7.3	8.5

[a] η_{rel} is the ratio of viscosities of solvent and D_2O. Reported uncertainties are standard deviations from four replicate measurements, and this error is less than 0.4×10^{-11} m^2/s for each value.

Chemicals. Ficoll 70 (Sigma, highest purity) was dissolved in 20 mM sodium phosphate buffer (pH 7.0). GuHCl and urea (Fisher Scientific, ultra pure) stock solutions were freshly prepared for each experiment in 20 mM sodium phosphate buffer (that was brought to pH 7.0); concentration was determined with a Zeiss refractometer.

Spectroscopic Methods. Absorption spectra were measured on a Cary 50 spectrophotometer (1 cm cell). Far-UV circular dichroism (CD) spectra (200−260 nm) of the protein samples were collected on a Chirascan (Applied Photophysics) and Jasco 810 CD spectropolarimeters with a 1 nm data interval in a 1 mm cell (thermal melts) and 1 cm cell (time-resolved experiments). Fluorescence measurements were performed on a Cary Eclipse fluorometer. Emission (excitation at 280 nm) was recorded from 290 to 400 nm with 1 nm data interval (3 mm and 1 cm cells). All measurements were performed at 20 °C unless otherwise stated. Spectra are averages of five scans, and all experiments were executed at least in triplicate.

NMR Diffusion. NMR samples were prepared by lyophilizing aqueous protein solutions and dissolving the dry product with D_2O solutions containing desired concentrations of denaturant (see Table 1). Samples were stored in a tube and plunger assembly (Shigemi) made of glass matching the magnetic susceptibility of water. Diffusion coefficients were measured at 25 °C on a Bruker DRX 600 NMR instrument fitted with a cryo TXI (^{1}H, ^{13}C, ^{15}N) 5 mm probe and a *z*-axis gradient system. For pulsed field gradient (PFG) diffusion measurements the bipolar stimulated echo sequence from the Bruker library was employed with a diffusion delay of 300 ms and bipolar gradient pulses of 12 ms (2 × 6 ms), and the gradient amplitude varied linearly in 32 steps between 0.7 and 18.5 G/cm. A total of 16 scans were accumulated with a recycle delay of 10 s. Each slice consists of 8K complex points and a sweep width of 16 ppm. Data were processed with Bruker Topspin vs 2.0. FIDs were zero filled to 16K complex points and apodized with a 10 Hz Lorentzian function. No baseline correction was performed. PFG experiments with the folded samples were repeated four times to obtain estimates of the uncertainty in the diffusion coefficient, *D*. The decays of the integrated protein resonances were fit to

single-exponential decay functions to determine D:

$$I(t) = I(0)\exp(-q^2(\Delta - \delta/3)D)$$

Here q ($= 2\pi\gamma\delta G$; where γ is the gyromagnetic ratio of ^{1}H) is the experimental variable (leading to a decay) proportional to the pulsed field gradient, G; Δ is the diffusion delay, and δ is the length of the gradient pulse.

Thermal Unfolding. Thermally induced unfolding of cpn10 in presence and absence of 300 mg/mL Ficoll 70 was monitored via CD at 230 nm from 20 to 90 °C with a scan rate of 1 °C/min. Scan rates from 2 to 0.5 °C/min were tested; it was found that samples had reached equilibrium at each point when using 1 °C/min or slower speeds. Protein concentration ranged between 5 to 100 μM. Protein samples were also reheated a second time which gave the same thermal profiles as the first heating, in both the absence and presence of Ficoll 70. This implies reversibility. The thermal unfolding curves were fitted to a modified form of the van't Hoff equation, which simultaneously fits the folded and unfolded baselines and the transition region to obtain the thermal midpoint (T_m) values for unfolding at each solvent condition.[48,49] The ΔH values obtained through the fits were not used as they correspond to two-state unfolding, not a folded heptamer to seven unfolded monomers reaction.

Chemical Unfolding. Chemical denaturation of cpn10 (without and with 300 mg/mL Ficoll 70) was performed at 20 °C (pH 7.0) using GuHCl (in 0.5 M increments) as denaturant. Samples were fixed to a final protein concentration of 20, 60, and 100 μM cpn10 and were incubated for 2 h before measurements. Unfolding was followed by far-UV CD and fluorescence detections. Each transition was analyzed using the following mechanism ($F_{oligomer}$, folded oligomer; $U_{monomer}$, unfolded monomer) an apparent two-state reaction coupled to dissociation:

$$F_{oligomer} \rightleftharpoons 7U_{monomer}$$

The equilibrium constant, $K_{unf,diss}$, and the free energy change, $\Delta G^{0'}_{unf,diss}$, are defined as

$$K_{unf,diss} = [U_{monomer}]^7/[F_{oligomer}] \quad \text{and}$$

$$\Delta G^{0'}_{unf,diss} = -RT \ln K_{unf,diss}$$

$[F_{oligomer}]$ is the concentration of folded oligomers (in M), and $[U_{monomer}]$ is the concentration of unfolded monomers (in M) at each denaturant concentration. R is the gas constant, and T is the absolute temperature. The free energy change can be expressed as a function of denaturant concentration:

$$\Delta G^{0'}_{unf,diss} = \Delta G^{0'}_{unf,diss}(H_2O) - m[\text{denaturant}]$$

In this equation, m describes the sensitivity of the transition to denaturant.[50] $\Delta G^{0'}_{unf,diss}(H_2O)$ is the free energy of unfolding in aqueous solution at pH 7 (in this case per mole of oligomer), and the superscript 0′ indicates a modified standard state.

Time-resolved unfolding experiments were performed by manual mixing of folded protein (20 μM cpn10) with denaturant at different final concentrations that favored the unfolded/dissociated form (2.5−4 M GuHCl). The samples were prepared in the absence and presence of Ficoll 70 (150 and 300 mg/mL). The CD signal at 230 nm was followed as function of time for up to 50 min. All experiments were carried out at 20 °C. The dead time in these experiments was roughly 10 s. The kinetic traces were fit to single-exponential decay equations to extract the rate constants.

Cross-Linking. Reagents for cross-linking were purchased from Sigma. Stock solutions of urea and GuHCl were mixed with cpn10 solutions (with and without 300 mg/mL Ficoll 70) to give a fixed concentration of 20 μM protein at different denaturant concentration (final volume 100 μL). Samples were allowed to equilibrate for 2 h at 20 °C before addition of 5 μL of 25% (v/v) glutaraldehyde (Sigma). After 2 min incubation, the reactions were quenched by addition of 10 μL of 1 M $NaBH_4$, 0.1 N NaOH. Following 20 min further incubation, the cross-linked cpn10 solutions were precipitated with trichloroacetic acid (10% v/v) (Sigma). The resulting pellets were analyzed by sodium dodecyl sulfate polyacrylamide gel electrophoresis (SDS-PAGE) using a precast ClearPAGE 16% gel (CBS Scientific). Gel Doc EZ system (Bio Rad) was used for making analysis and imaging of the gels.

Heptamer−Monomer Equilibrium. Measurements of fluorescence changes linked to heptamer-to-monomer dissociation were probed by monitoring tyrosine fluorescence as a function of cpn10 concentration. Cpn10 samples were prepared at various concentrations (0.5−12 μM) in the absence and presence of 300 mg/mL Ficoll 70. Samples were incubated overnight at 20 °C, and the fluorescence was measured (excitation at 280 nm). The heptamer−monomer transition data were analyzed as described in the Supporting Information.

Chemical Data Analysis. The equilibrium unfolding data with and without Ficoll 70 as a function of GuHCl were analyzed as described in the Supporting Information. In short, the complete CD or fluorescence spectra at each condition were used to extract unfolding curves at each wavelength. The reliability of fitting each of these around 50 transitions was then used to select a range of wavelengths that gave reliable data. This data set was then used to extract thermodynamic parameters. The same procedure was used to analyze the fluorescence spectra linked to the heptamer−monomer dissociation reaction (Supporting Information).

GuHCl/Urea Concentration Corrections. An inert crowding agent increases the concentration of any small solute by decreasing its available volume through steric repulsion (assuming no interactions between the crowding agent and the solute).[51−53] The GuHCl/urea concentration in the cpn10 samples were therefore corrected ($[\text{denaturant}]_{corr}$) to account for the solvent-excluded volume due to the presence of Ficoll. For this, we determined the value of Ficoll 70's partial specific volume to be 0.65 ± 0.02 mL/g. In short, a specific amount of Ficoll powder was added to a volumetric flask, and the weight was measured. Water or buffer was then added to fill up to the specified volume. The weight was measured again, and from this, it could be calculated how much water had to be added to create the specified volume. From this, the volume occupied by Ficoll per mass unit could be calculated. The partial specific volume value for Ficoll did not depend on the amount of crowding agent dissolved (200−400 mg/mL final concentration). Moreover, the crowding agent's partial specific volume value was the same in buffer, in 0.5−8 M GuHCl and in 10 M urea (here, premade stock solutions of the denaturants, 0.5−8 and 10 M, respectively, were used instead of water in the above experiment). For corrections, we used $[\text{denaturant}]_{corr} = (1/f_{av})[\text{denaturant}]$, where f_{av} is the volume fraction available to the solvent.[51] For example, for 300 mg/mL Ficoll 70 solutions, f_{av} is about 0.8 (i.e., $1 - [0.65\ \text{mL/g} \times 0.3\ \text{g/mL}]$). All GuHCl/urea concentrations used in the chemical denaturant experiment with 300 mg/mL

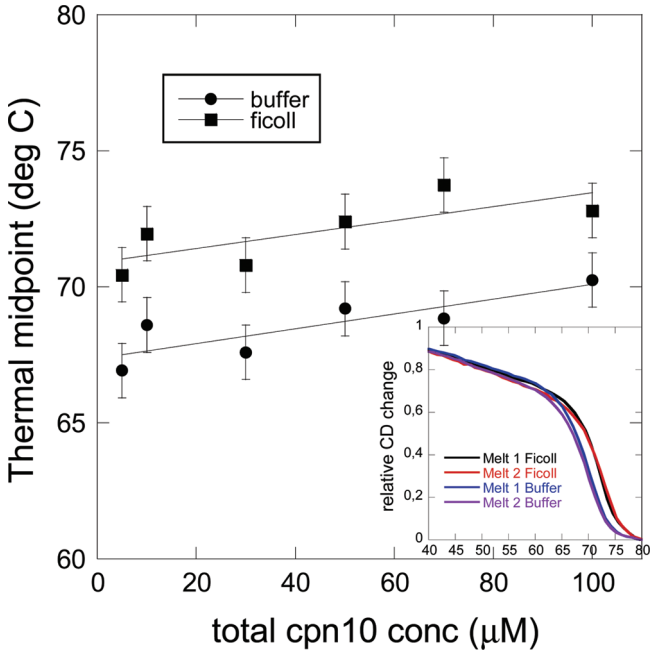

Figure 2. Thermal midpoints as a function of cpn10 concentration, with and without 300 mg/mL Ficoll 70. Errors are estimated from 2 to 4 separate experiments. Solid lines are linear fits and are included to illustrate the protein-concentration-dependent stabilization of cpn10 at both conditions. Inset: unfolding curves for repeated experiments (melts 1 and 2) with the same sample demonstrating reversibility in buffer and in Ficoll 70, respectively.

Ficoll 70 were corrected in this way based on the amount of crowding agent present.

RESULTS

Choice of Protein and Crowding Agents. Cpn10 (Figure 1) was selected as the target oligomer since it is one of few known oligomeric proteins that fold and unfold reversibly *in vitro*. There is also a large set of data on its properties in dilute buffer conditions.[39−41,54−57] The crowding agent selected for this study is the sugar-based polymer Ficoll 70 (MW of 70) since (a) it is believed to affect proteins via excluded volume effects, (b) it has low absorption above 200 nm enabling spectroscopic studies, (c) it is inert and does not have phase transitions in the temperature regions to be studied, and (d) Ficoll appears to adopt a semirigid spherical shape at dilute conditions.[58−62]

Effects on Thermal Stability. Cpn10 thermal denaturation was probed by far-UV CD at 230 nm. Cpn10 unfolds in a reversible, cooperative transition in buffer when the temperature is raised (inset, Figure 2). The thermal midpoints are protein-concentration-dependent (more protein, the higher the thermal midpoint), in accord with a coupled unfolding/dissociation equilibrium unfolding process.[41] When 300 mg/mL Ficoll 70 is present in the solutions, the thermal transition is shifted to higher temperatures at all protein concentrations (Figure 2). On average, the thermal midpoint is increased by 3°−4° in presence of Ficoll 70 as compared to in buffer.

Effects on Folded and Unfolded States Secondary Structures. Earlier studies on some small marginally stable proteins have shown that the folded state secondary structure is modulated by macromolecular crowding.[23,24] To test this possibility for cpn10, we compared the far-UV CD signal (Figure 3A) and the tyrosine emission (Figure 3B) for folded and unfolded (using GuHCl as well as urea as chemical denaturants) states of cpn10 without and with 300 mg/mL Ficoll 70. We note that cpn10 has an abnormal far-UV CD signal that is dominated by a positive tyrosine-induced peak at 230 nm.[41] The negative signal at 210−220 nm is weak as cpn10 has many unstructured loops and short β-strands. There appears to be no difference on the secondary structure level due to the presence of Ficoll 70 in the folded assembled state. In the unfolded state, the CD data imply random coil in both conditions. In terms of fluorescence, the folded state emission is somewhat quenched by the presence of Ficoll 70, although the decreased emission of the unfolded state is similar with and without Ficoll 70.

Nature of Unfolded State in Denaturants. Earlier work had postulated an "assembled but unfolded" denatured state for cpn10 in urea[41] although in GuHCl, the denatured state corresponded to unfolded monomers. The evidence came from gluteraldehyde cross-linking experiments, however, performed after only 10 min incubation, which we find is too short to complete unfolding at all conditions (2 h incubation required at most conditions at room temperature). We have now performed a new set of cross-linking experiments of cpn10 as a function of urea and GuHCl concentrations, respectively, without and with 300 mg/mL Ficoll 70 (Figure 4A−D). It is clear from the data that cpn10 unfolds and dissociates in a cooperative and coupled process in both chemical denaturants and regardless of if Ficoll 70 is present or not. However, it is apparent from the gels that Ficoll shifts the unfolding/dissociation equilibrium to higher denaturant concentrations (i.e., has a stabilizing effect).

To further confirm that the unfolded state is monomeric, we performed diffusion experiments using NMR.[63] For this, we used dioxane as a internal standard to correct for viscosity changes and the monomeric protein S16 (104 residues) as a model of a monomeric globular protein.[64] Whereas the diffusion constant for S16 decreases upon unfolding due to the larger hydrodynamic radius of an unfolded polypeptide, the diffusion constant for cpn10 increases upon unfolding (Table 1). This direction of the change implies that the unfolded cpn10 molecules are *smaller* than the folded molecule; this is compatible with dissociation into monomers upon unfolding. Notably, the diffusion constants for unfolded cpn10 and unfolded S16 are similar in magnitude, which further supports a monomeric unfolded state for cpn10 as the cpn10 and S16 peptides are similar in size (102 vs 104 residues). If cpn10 had remained heptameric upon unfolding, the diffusion constant should have decreased in the denaturant conditions. Thus, from the data in Table 1, it is clear that cpn10 is monomeric in both high concentrations of urea and GuHCl, in good agreement with the cross-linking data.

Chemically Induced Unfolding. GuHCl was used as chemical denaturant, and cpn10 stability was probed at different protein concentrations, with and without 300 mg/mL Ficoll 70. To accurately analyze the data, we developed a new approach that in essence uses the whole spectra (CD or fluorescence spectra) and derives an unfolding curve at each wavelength (Figure 5). From Levenberg−Marquart error estimates at each wavelength, an appropriate range of wavelengths are then selected that exhibits errors below a certain threshold. We selected to include all data sets with standard deviation (SD) less or equal to 2.5 times the lowest SD (explanation for this

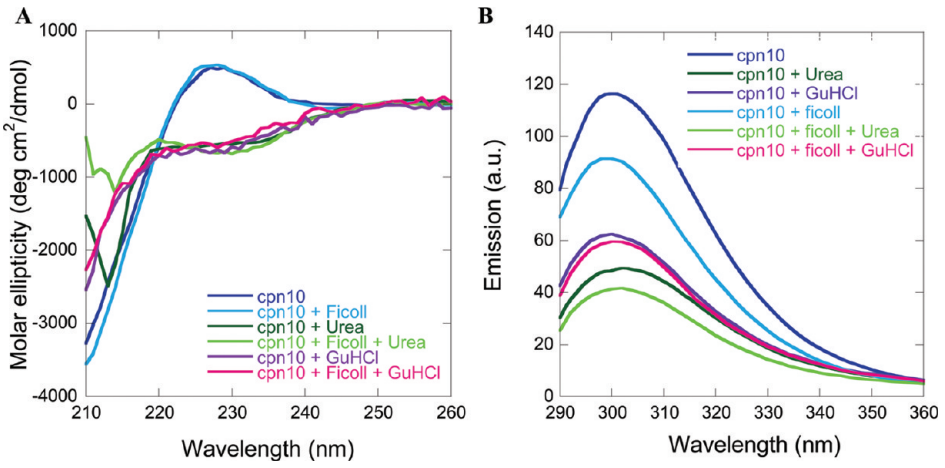

Figure 3. Folded and unfolded (in 7 M urea and 3 M GuHCl, respectively) far-UV CD signals (A) and tyrosine emission (B) for cpn10 without and with 300 mg/mL Ficoll 70 (60 μM protein, 20 °C).

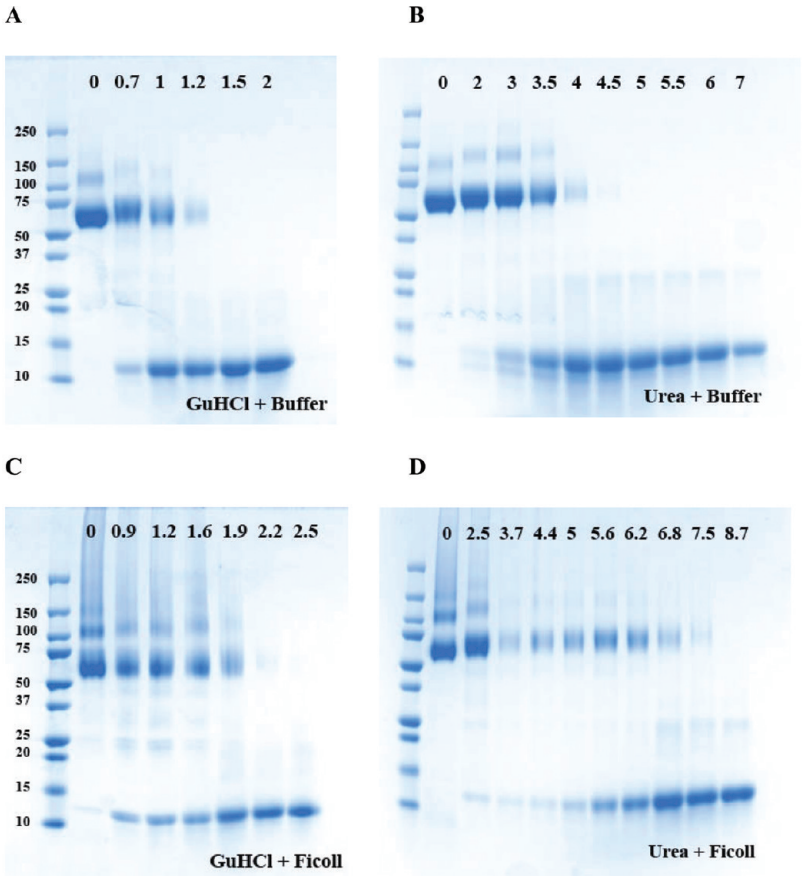

Figure 4. SDS-PAGE of cpn10 cross-linked with glutaraldehyde with and without 300 mg/mL Ficoll 70 after induced incubation with GuHCl (A, C) and urea (B, D). Numbers indicate the concentration of denaturant (in M) in the experiments. 20 μM cpn10 was used in all the reactions (20 °C).

choice is given in the Supporting Information). The unfolding curves within this selected set of wavelengths are then used to derive midpoints and unfolding free energies (and their errors) for each condition (Figure 5). This procedure is explained in detail in the Supporting Information. The GuHCl data were analyzed using a "folded heptamer" to "seven unfolded monomers" transition, i.e., F_7 to 7U, based on the experiments described in the previous section. We also tested several other mechanisms, but in fact, the F_7 to 7U mechanism fitted the data best (notably in this mechanism the transition should be curved less in the beginning of the cooperative transition as compared to in the end, which is experimentally seen).

In Figure 6, we show fitted transition midpoints (Figure 6A) and $\Delta G^{0'}_{unf/diss}(H_2O)$ values (Figure 6B) for three different

dx.doi.org/10.1021/bi2002086 |*Biochemistry* 2011, 50, 3034–3044

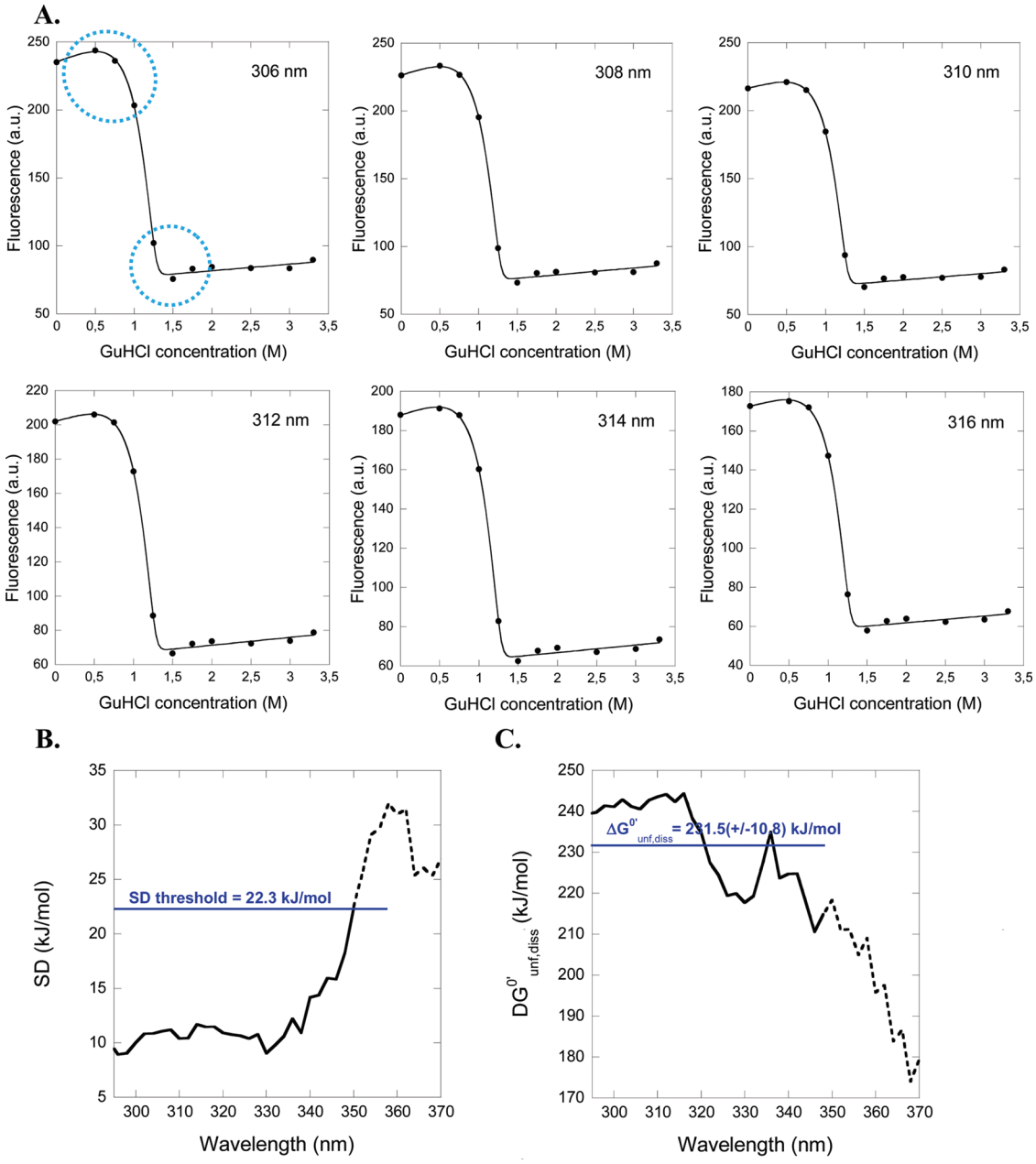

Figure 5. Matlab analysis of cpn10 unfolding curves based on $F_7 \rightleftharpoons 7U$ mechanism (see Supporting Information). (A) Examples of unfolding traces created from fluorescence data at different wavelengths (in total unfolding curves at 52 wavelengths were analyzed; 294−396 nm although data above 370 nm was too poor and not included in analysis shown here). The shown data are for GuHCl-induced unfolding of 100 μM cpn10 in buffer. Note that the $F_7 \rightleftharpoons 7U$ fits are less curved in the beginning of the cooperative transition as compared to in the end (emphasized by blue circles). (B) Standard deviations in Gibbs free energy from the $F_7 \rightleftharpoons 7U$ values using the Levenberg−Marquart algorithm. The lowest standard deviation in this data set was 8.9 kJ/mol (at 296 nm). Wavelengths with standard deviations in their $\Delta G^{0'}_{unf,diss}(H_2O)$ fits lower than 2.5 × 8.9 kJ/mol = 22.3 kJ/mol were selected as "good". In this data set 28 wavelengths were found below the threshold (solid curve; 294−348 nm). (C) $\Delta G^{0'}_{unf,diss}(H_2O)$ shown as a function of wavelength. The wavelength region with SD in the acceptable range (determined in (B)) is used to derive the average $\Delta G^{0'}_{unf,diss}(H_2O)$ value and standard deviation (based on these 28 data points).

cpn10 protein concentrations, with and without 300 mg/mL Ficoll 70, for GuHCl-induced reactions (data summarized in Table S1, Supporting Information). The midpoints are increased in GuHCl due to the presence of Ficoll 70 (~0.5 M), and the magnitude appears independent of protein concentration. This midpoint trend correlates well with the thermal data showing that T_m is increased in Ficoll 70 (Figure 2). In parallel with the increased midpoints, the free energy for coupled unfolding/dissociation is increased in Ficoll 70 by on average 20−30 kJ/mol (average free energy of the heptamer is 239 kJ/mol in buffer and 275 kJ/mol in Ficoll 70).

The transition midpoints are found to increase as a function of increased protein concentration in both the buffer and the Ficoll 70 set of data. This trend is expected based on the proposed mechanism involving only folded heptamers and unfolded monomers and Le Chatelier's principle. As reported before, the

dx.doi.org/10.1021/bi2002086 |*Biochemistry* 2011, 50, 3034–3044

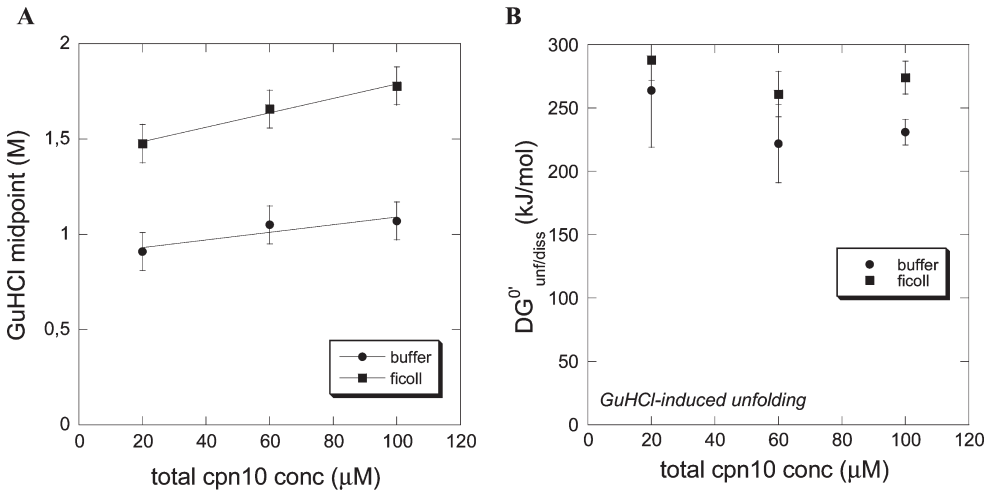

Figure 6. Transition midpoints (A) and $\Delta G^{0'}_{unf,diss}(H_2O)$ (B) (analysis based on "one folded heptamer" to "seven unfolded monomers" reaction) values for GuHCl-induced unfolding as a function of cpn10 concentration and presence or not of 300 mg/mL Ficoll 70. Denaturant concentrations are corrected for solvent excluded volume in the Ficoll experiments. Error bars come from the complete data analysis presented in the Supporting Information.

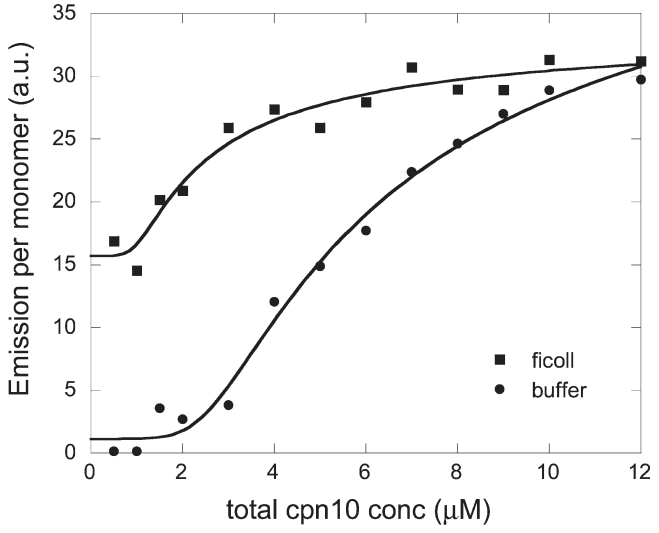

Figure 7. Heptamer−monomer transitions as a function of protein concentration in buffer and in 300 mg/mL at 20 °C (data at 302 nm shown). The heptamer has higher emission, per monomer unit, than the monomers, and this is used to find the heptamer−monomer midpoint concentration (defined as the monomer concentration where half of the polypeptides are monomers and the other half form heptamers) and the heptamer−monomer dissociation constant. See Supporting Information for details of spectral analysis. The solid lines are fits to a heptamer−monomer equilibrium equation (see Supporting Information). We note that the fit for the monomer−heptamer transition in buffer appears to reach a higher final emission at cpn10 concentrations higher than 12 μM than the transition in Ficoll; this is in accord with the difference in the emission spectra in Figure 3B (collected at 60 μM).

extrapolated free energy of cpn10 unfolding/dissociation becomes independent of protein concentration.[41]

Effect on Heptamer−Monomer Dissociation Constant. The heptamer−monomer equilibrium constant was assessed by fluorescence changes as previously reported.[41] In practical, the protein is diluted stepwise and the fluorescence per concentration unit is compared as a function of total protein concentration. Whereas heptamers have higher fluorescence per concentration unit, monomers have less emission per concentration unit, and an equilibrium dissociation constant can be assigned in the transition between these two conditions. Fluorescence as a function of cpn10 concentration was probed in buffer and 300 mg/mL Ficoll 70 (Figure 7). Also, here the full spectra were used for analysis (see Supporting Information). There is a difference between the curves, indicating that the corresponding heptamer−monomer K_D value in Ficoll is lower than in buffer (i.e., tighter binding in Ficoll). Data analysis (Supporting Information) provides heptamer−monomer transition midpoints at 3.1 ± 0.5 and 8.1 ± 0.1 μM (i.e., the concentrations where 50% of monomers are found as monomers and 50% of monomers are found as heptamers) total cpn10 monomer concentrations, for Ficoll and buffer conditions, respectively. See Table S2 of the Supporting Information for complete data. These values correspond to a heptamer−monomer dissociation free energy, $\Delta G^{0'}_{diss}$ ($= -RT \ln K_D$), of 191 ± 2.3 and 177 ± 0.2 kJ per mol of heptamer, respectively.

Effect on Unfolding Kinetics. To assess if the increased thermodynamic stability for the heptamer in the equilibrium experiments in Ficoll 70 (i.e., $\Delta\Delta G_{0,unf/diss}$ of 36 kJ/mol heptamer) arises due to changes in unfolding kinetics, we performed a set of kinetic experiments in GuHCl without and with various amounts of Ficoll 70. At least three observations can be made from the data in Figure 8. (1) Cpn10 unfolding/disassembly is slower in the presence of Ficoll 70. (2) The decrease in the unfolding rate constants scales with the amount of Ficoll 70; i.e., the more Ficoll present, the slower the rate constants. (3) The slopes of the ln $k_{unf/diss}$ data at the various conditions are roughly equal, indicating no major change in the mechanism/transition state structure due to Ficoll 70. Comparing the buffer and 300 mg/mL Ficoll kinetic data at specific denaturant concentrations (i.e., vertical comparisons in Figure 8), it emerges that the energetic effect arising from different unfolding kinetics is roughly 5 kJ/mol of heptamer (i.e., RT[ln $k_{unf/diss}$(buffer, X M denaturant) − ln $k_{unf/diss}$(Ficoll, X M denaturant)]). Thus, there must be kinetic effects on folding/assembly reactions, too, to account for the total amount of thermodynamic stabilization by Ficoll 70 (36 kJ/mol of heptamer).

dx.doi.org/10.1021/bi2002086 |*Biochemistry* 2011, 50, 3034–3044

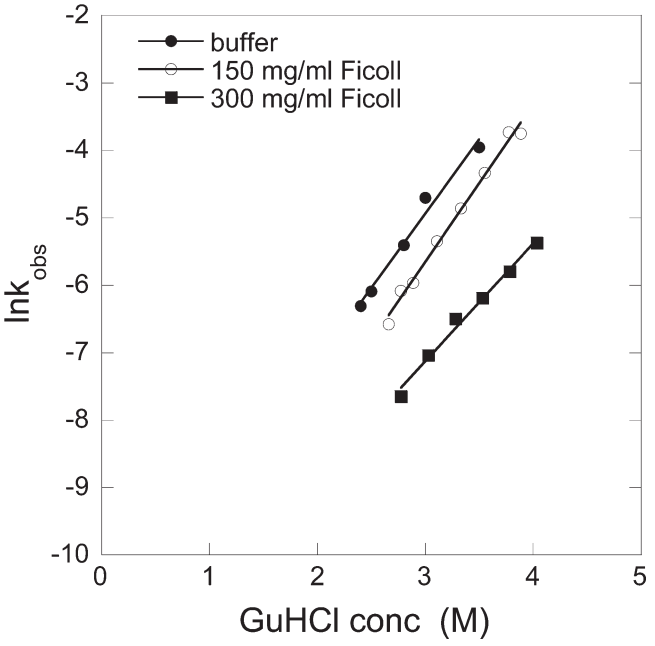

Figure 8. Unfolding kinetics of cpn10 without and with various amounts of Ficoll 70 at 20 °C probed by CD changes (20 μM cpn10) in GuHCl.

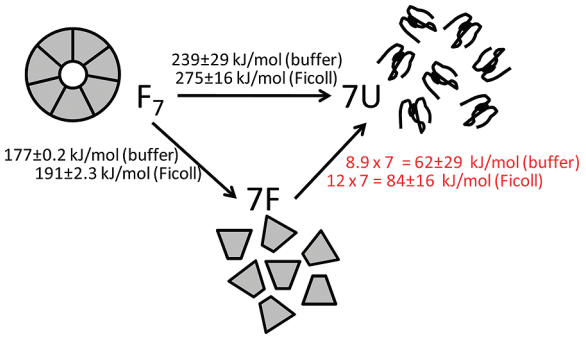

Figure 9. Thermodynamic scheme linking cpn10 heptamer unfolding/dissociation (as induced by chemical denaturants) with heptamer disassembly into folded monomers (as induced by dilution below K_D) and monomer unfolding. Using our experimental free energy values in buffer and in Ficoll 70 (at 20 °C) for heptamer unfolding/dissociation (GuHCl data; protein concentration independent) and for heptamer disassembly to folded monomers, cpn10 monomer stability in buffer and in Ficoll 70 can be predicted. It emerges that the monomers are largely stabilized in Ficoll 70 (by 33%; 9 vs 12 kJ/mol in buffer vs Ficoll 70). In contrast, each monomer−monomer interface is only stabilized by about 8% in Ficoll (25 vs 27 kJ/mol in buffer vs Ficoll 70).

DISCUSSION

We have here studied the effect of a macromolecular crowding agent, Ficoll 70, on the stability and assembly of a heptamer, cpn10. Cpn10 is a useful system for thermodynamic analysis since many other protein oligomers unfold irreversibly *in vitro*. The bacterial version of cpn60, GroEL, does not refold spontaneously to its tetradecameric form from unfolded monomers, but the presence of crowding agents was found to improve both speed and yield of refolding.[65] Since higher organisms have a large fraction of proteins that functions in homo- and hetero-oligomeric forms, oligomers are an important class of proteins to study. From an overall glance of our findings, it appears that macromolecular crowding does not have radically different thermodynamic effects on a heptamer as compared to on monomeric proteins.

In both thermal and chemical equilibrium experiments, cpn10 unfolding is coupled to protein−protein dissociation in an apparent two-state, folded-heptamer-to-unfolded-monomers, process. From the current study, we conclude that the presence of Ficoll 70 does not affect the folded state secondary structure or the unfolded state, as probed by far-UV CD (Figure 3); in addition, cross-linking and NMR diffusion experiments support that the folded heptamer remains a heptamer in Ficoll 70 and that the unfolded state in denaturants is monomeric also in the presence of Ficoll 70 (Figure 4). Thus, the apparent two-state mechanism for equilibrium denaturation of cpn10 is retained in Ficoll 70. Nonetheless, the heptamer is stabilized toward thermal perturbation by the presence of Ficoll 70. The T_m is increased by about 3−4 °C in 300 mg/mL Ficoll 70 (Figure 2). This is in the range of theoretical predictions[66] and values found for monomeric proteins.[17,23,24,67,68]

The cpn10 heptamer chemical stability is also increased in Ficoll 70 as compared to in buffer (Figure 6). The coupled unfolding dissociation free energy increases by about 15% in Ficoll 70 as compared to in buffer. To deconvolute the effect of Ficoll 70 into contributions from monomer stability and monomer−monomer interfaces, we assessed the heptamer−monomer dissociation constant in buffer versus in Ficoll 70 (Figure 7). From the measured thermodynamic data on chemical unfolding/dissociation and on heptamer dissociation, with and without Ficoll, we prepared a thermodynamic cycle that predicts the monomer stability in buffer and in Ficoll 70 (Figure 9). It emerges that the presence of Ficoll 70 stabilizes individual monomers by about 33% (12 vs 9 kJ/mol monomer). This should be compared to a roughly 8% stabilization of the interfaces by the presence of Ficoll 70 (27 vs 25 kJ/mol interface). The monomers are less stable than the interfaces; in the current experiments in buffer, the interfaces contribute with 75% of the overall heptamer stability and the subunits with the remaining 25%. Thus, in agreement with previous conclusions,[67] crowding exerts larger effects on the species (here, the individual monomers) with the lower thermodynamic stability. Another way to analyze the numbers is to divide the increase in heptamer stability (36 kJ/mol heptamer) between that involved in the interfaces (14/36 kJ/mol, i.e., 39%) and that in monomers (22/36 kJ/mol, i.e., 61%). Thus also in absolute values are monomers stabilized more than the interfaces.

In agreement with the heptamer−monomer dissociation experiments, it is expected that the heptamer is favored (over the monomers) at crowded conditions as it should account for less covolume than seven individual monomers. To ensure that this assumed trend in covolumes is correct, we calculated the covolume[69] of the monomeric unit, assuming a sphere radius of 11 Å, and the heptamer, assuming a cylinder (central cavity is too small for Ficoll to penetrate), with dimensions taken from the crystal structure (36 Å radius of cross section, 22 Å height) and using a probe sphere matching Ficoll 70 (i.e., radius of 55 Å). From this simplified calculation, seven monomers take up roughly 3 times more volume than the heptamer. We want to note, however, that the shape of Ficoll 70 is likely not a sphere at our conditions; several different structures have been proposed.[62,70,71] It is also possible that the shape of Ficoll is affected by the denaturants[72] although Ficoll's partial specific volume did not change with denaturants. Importantly, in our experiments, no assumptions of the shape of Ficoll 70 are made.

There are a few experimental reports of actual magnitudes of macromolecular crowding effects on protein cooperative assembly/disassembly. In Minton's recent study on catalase and superoxide dismutase interactions, the maximal difference in heterodimer K_D was a factor 20 for 300 mg/mL of crowding agents.[18] In another study of the SARS-CoV 3CL peptidase dimer, no effect on K_D by 100 mg/mL PEG was found.[73] Similarly, no effect by crowding agents was found on the assembly of the TEM1−BLIP pair as well as of the barnase−barstar pair.[74] Still experimentally and computationally determined increases in protein−protein affinity due to macromolecular crowding or confinement have been reported.[13,14,75,76] The BPTI monomer−decamer equilibrium constant was found to increase by a factor of 500000 (corresponding to about 130 kJ/mol) using a magnetic relaxation dispersion method.[77] In the recent dynamic molecular model of the bacterial cytoplasm, dimer K_D values were predicted to increase on average 5-fold (corresponding to about 4 kJ/mol), whereas the calculations suggested increases in K_D values by up to 5000−10000-fold for two eightmers (corresponding to about 20 kJ/mol).[78] Although our difference in free energy of assembly with and without crowding is only 8% of the total free energy (absolute difference is 14 kJ/mol), this corresponds to heptamer−monomer K_D values that differ by a factor of 300. Thus, our K_D result falls in between the predictions made for dimers and eightmers in the study by Elcock.[78] The protein concentrations used in the K_D experiments (here and in all mentioned studies above) are based on the total volume, not accounting for excluded volume. Thus, the "crowding effect" will include one component that is related to a change in protein concentration simply due to less available space and another component that is due to the excluded volume effect making smaller species more favorable.

Effects of crowding on protein noncooperative self-assembly have also been reported. For example, it has been shown that the indefinite linear self-association of the bacterial cell division protein FtsZ is stimulated by the presence of "crowder" proteins.[79] Also, both fibrinogen and tubulin self-associate in crowded conditions.[79] For the HIV-1 capsid protein CA, *in vitro* polymerization is normally only observed at high ionic strength. However, crowding agents were found to induce fast and efficient polyermisation of CA even at low (physiological) ionic strength.[80]

The stabilizing effect of macromolecular crowding for the cpn10 heptamer is in part due to slower unfolding kinetics in Ficoll 70 (Figure 8). This is similar to observations made for the monomeric CRAB 1 protein in the presence of Ficoll 70.[81] Like for cpn10, CRAB1 unfolding was retarded without change in the urea dependence. This was interpreted as no appreciable change in the nature of the transition state. Refolding kinetics of CRAB1 in the presence of Ficoll 70 was not studied due to the reaction's complexity; likewise, cpn10 refolding is an intricate process as it involves both assembly and folding steps, and parallel paths have been reported.[55] Although we did not measure cpn10 refolding with Ficoll 70, it is obvious that Ficoll 70 acts to accelerate parts of this process.

CONCLUSIONS

Proteins fold in a cell's environment that is crowded with macromolecules. This crowded environment will cause excluded volume effects, weak interactions, and hydrodynamic effects.[82] It is therefore important to understand—on a molecular level—how these factors affect protein biophysical properties in comparison to their behaviors in conventional experiments performed in dilute buffers *in vitro*. We here report the effects of excluded volume on a protein heptamer, cpn10. We find that the effects of macromolecular crowding on cpn10 are similar in magnitude to effects found on monomeric proteins. Since the observed effects are small, it appears that conclusions drawn from *in vitro* biophysical studies of protein complexes likely will hold true also at *in vivo* conditions. As a complement, we describe a new multiwavelength approach to analyze spectroscopic data that results in more accurate analysis than conventional single-wavelength analysis: this approach will be applicable to many other studies.

ASSOCIATED CONTENT

Supporting Information. Data analysis; Tables S1and S2. This material is available free of charge via the Internet at http://pubs.acs.org.

AUTHOR INFORMATION

Corresponding Author

*Ph: +46-90-778400. Fax: +46-90-7867655. E-mail: pernilla.wittung@chem.umu.se.

Funding Sources

This work was supported by the Kempe (M.W.W., C.F.W., and P.W.S.), Göran Gustafsson (P.W.S.), and Wallenberg (P.W.-S.) foundations, Umeå University Young Researcher Awards (M.W.W. and P.W.S.), and the Swedish Research Council (P.W.S., M.W.W.).

ACKNOWLEDGMENT

We thank Margaret Cheung for covolume calculations and useful discussions and Alexander Schug for preparation of Figure 1.

ABBREVIATIONS:

CD ,circular dichroism; T_m ,thermal midpoint; NMR ,nuclear magnetic resonance; cpn10 ,co-chaperonin protein 10

REFERENCES

(1) Rivas, G., Ferrone, F., and Herzfeld, J. (2004) Life in a crowded world. *EMBO Rep. 5*, 23–27.

(2) Ellis, R. J., and Minton, A. P. (2003) Cell biology: join the crowd. *Nature 425*, 27–28.

(3) Minton, A. P., and Wilf, J. (1981) Effect of macromolecular crowding upon the structure and function of an enzyme: glyceraldehyde-3-phosphate dehydrogenase. *Biochemistry 20*, 4821–4826.

(4) Laurent, T. C., and Ogston, A. G. (1963) The Interaction between Polysaccharides and Other Macromolecules. 4. the Osmotic Pressure of Mixtures of Serum Albumin and Hyaluronic Acid. *Biochem. J. 89*, 249–253.

(5) Minton, A. P. (2005) Models for excluded volume interaction between an unfolded protein and rigid macromolecular cosolutes: macromolecular crowding and protein stability revisited. *Biophys. J. 88*, 971–985.

(6) Zhou, H. X. (2004) Loops, linkages, rings, catenanes, cages, and crowders: entropy based strategies for stabilizing proteins. *Acc. Chem. Res. 37*, 123–130.

(7) Cheung, M. S., Klimov, D., and Thirumalai, D. (2005) Molecular crowding enhances native state stability and refolding rates of globular proteins. *Proc. Natl. Acad. Sci. U.S.A. 102*, 4753–4758.

(8) Cheung, M. S., and Thirumalai, D. (2007) Effects of crowding and confinement on the structures of the transition state ensemble in proteins. *J. Phys. Chem. B 111*, 8250–8257.

(9) Homouz, D., Sanabria, H., Waxham, M. N., and Cheung, M. S. (2009) Modulation of calmodulin plasticity by the effect of macromolecular crowding. *J. Mol. Biol. 391*, 933–943.

(10) Zhang, S. Q., and Cheung, M. S. (2007) Manipulating biopolymer dynamics by anisotropic nanoconfinement. *Nano Lett. 7*, 3438–3442.

(11) Qin, S., and Zhou, H. X. (2009) Atomistic modeling of macromolecular crowding predicts modest increases in protein folding and binding stability. *Biophys. J. 97*, 12–19.

(12) Mittal, J., and Best, R. B. (2008) Thermodynamics and kinetics of protein folding under confinement. *Proc. Natl. Acad. Sci. U.S.A. 105*, 20233–20238.

(13) Wang, W., Xu, W. X., Levy, Y., Trizac, E., and Wolynes, P. G. (2009) Confinement effects on the kinetics and thermodynamics of protein dimerization. *Proc. Natl. Acad. Sci. U.S.A. 106*, 5517–5522.

(14) Griffin, M. A., Friedel, M., and Shea, J. E. (2005) Effects of frustration, confinement, and surface interactions on the dimerization of an off-lattice beta-barrel protein. *J. Chem. Phys. 123*, 174707.

(15) McGuffee, S. R., and Elcock, A. H. (2006) Atomically detailed simulations of concentrated protein solutions: the effects of salt, pH, point mutations, and protein concentration in simulations of 1000-molecule systems. *J. Am. Chem. Soc. 128*, 12098–12110.

(16) Dedmon, M. M., Patel, C. N., Young, G. B., and Pielak, G. J. (2002) FlgM gains structure in living cells. *Proc. Natl. Acad. Sci. U.S.A. 99*, 12681–12684.

(17) Sasahara, K., McPhie, P., and Minton, A. P. (2003) Effect of dextran on protein stability and conformation attributed to macromolecular crowding. *J. Mol. Biol. 326*, 1227–1237.

(18) Jiao, M., Li, H. T., Chen, J., Minton, A. P., and Liang, Y. (2010) Attractive protein-polymer interactions markedly alter the effect of macromolecular crowding on protein association equilibria. *Biophys. J. 99*, 914–923.

(19) Crowley, P. B., Brett, K., and Muldoon, J. (2008) NMR spectroscopy reveals cytochrome c-poly(ethylene glycol) interactions. *ChemBioChem 9*, 685–688.

(20) Li, C., and Pielak, G. J. (2009) Using NMR to distinguish viscosity effects from nonspecific protein binding under crowded conditions. *J. Am. Chem. Soc. 131*, 1368–1369.

(21) Minton, A. P. (1983) The effect of volume occupancy upon the thermodynamic activity of proteins: some biochemical consequences. *Mol. Cell. Biochem. 55*, 119–140.

(22) Comper, W. D., and Laurent, T. C. (1978) An estimate of the enthalpic contribution to the interaction between dextran and albumin. *Biochem. J. 175*, 703–708.

(23) Perham, M., Stagg, L., and Wittung-Stafshede, P. (2007) Macromolecular crowding increases structural content of folded proteins. *FEBS Lett. 581*, 5065–5069.

(24) Stagg, L., Zhang, S. Q., Cheung, M. S., and Wittung-Stafshede, P. (2007) Molecular crowding enhances native structure and stability of alpha/beta protein flavodoxin. *Proc. Natl. Acad. Sci. U.S.A. 104*, 18976–18981.

(25) Homouz, D., Perham, M., Samiotakis, A., Cheung, M. S., and Wittung-Stafshede, P. (2008) Crowded, cell-like environment induces shape changes in aspherical protein. *Proc. Natl. Acad. Sci. U.S.A. 105*, 11754–11759.

(26) Martin, J., Geromanos, S., Tempst, P., and Hartl, F. U. (1993) Identification of nucleotide-binding regions in the chaperonin proteins GroEL and GroES. *Nature 366*, 279–282.

(27) Todd, M. J., Boudkin, O., Freire, E., and Lorimer, G. H. (1995) GroES and the chaperonin-assisted protein folding cycle: GroES has no affinity for nucleotides. *FEBS Lett. 359*, 123–125.

(28) Burston, S. G., Weissman, J. S., Farr, G. W., Fenton, W. A., and Horwich, A. L. (1996) Release of both native and non-native proteins from a cis-only GroEL ternary complex. *Nature 383*, 96–99.

(29) Shtilerman, M., Lorimer, G. H., and Englander, S. W. (1999) Chaperonin function: folding by forced unfolding. *Science 284*, 822–825.

(30) Braig, K., Otwinowski, Z., Hegde, R., Boisvert, D. C., Joachimiak, A., Horwich, A. L., and Sigler, P. B. (1994) The crystal structure of the bacterial chaperonin GroEL at 2.8 A [see comments]. *Nature 371*, 578–586.

(31) Athanasas-Platsis, S., Somodevilla-Torres, M. J., Morton, H., and Cavanagh, A. C. (2004) Investigation of the immunocompetent cells that bind early pregnancy factor and preliminary studies of the early pregnancy factor target molecule. *Immunol. Cell Biol. 82*, 361–369.

(32) Cappello, F., Bellafiore, M., David, S., Anzalone, R., and Zummo, G. (2003) Ten kilodalton heat shock protein (HSP10) is overexpressed during carcinogenesis of large bowel and uterine exocervix. *Cancer Lett. 196*, 35–41.

(33) Slavotinek, A. M., and Biesecker, L. G. (2001) Unfolding the role of chaperones and chaperonins in human disease. *Trends Genet. 17*, 528–535.

(34) Hunt, J. F., Weaver, A. J., Landry, S. J., Gierasch, L., and Deisenhofer, J. (1996) The crystal structure of the GroES co-chaperonin at 2.8 A resolution. *Nature 379*, 37–45.

(35) Mande, S. C., Mehra, V., Bloom, B. R., and Hol, W. G. (1996) Structure of the heat shock protein chaperonin-10 of Mycobacterium leprae. *Science 271*, 203–207.

(36) Roberts, M. M., Coker, A. R., Fossati, G., Mascagni, P., Coates, A. R., and Wood, S. P. (1999) Crystallization, x-ray diffraction and preliminary structure analysis of Mycobacterium tuberculosis chaperonin 10. *AActa Crystallogr., Sect. D: Biol. Crystallogr. 55*, 910–914.

(37) Hunt, J. F., van der Vies, S. M., Henry, L., and Deisenhofer, J. (1997) Structural adaptations in the specialized bacteriophage T4 co-chaperonin Gp31 expand the size of the Anfinsen cage. *Cell 90*, 361–371.

(38) Numoto, N., Kita, A., and Miki, K. (2005) Crystal structure of the Co-chaperonin Cpn10 from Thermus thermophilus HB8. *Proteins 58*, 498–500.

(39) Guidry, J. J., Shewmaker, F., Maskos, K., Landry, S., and Wittung-Stafshede, P. (2003) Probing the Interface in a Human Co-Chaperonin Heptamer: Residues Disrupting Oligomeric Unfolded State Identified. *BMC Biochem. 4*, 14.

(40) Guidry, J. J., and Wittung-Stafshede, P. (2002) Low stability for monomeric human chaperonin protein 10: interprotein interactions contribute majority of oligomer stability. *Arch. Biochem. Biophys. 405*, 280–282.

(41) Guidry, J. J., Moczygemba, C. K., Steede, N. K., Landry, S. J., and Wittung-Stafshede, P. (2000) Reversible denaturation of oligomeric human chaperonin 10: denatured state depends on chemical denaturant. *Protein Sci. 9*, 2109–2117.

(42) Boudker, O., Todd, M. J., and Freire, E. (1997) The structural stability of the co-chaperonin GroES. *J. Mol. Biol. 272*, 770–779.

(43) Higurashi, T., Nosaka, K., Mizobata, T., Nagai, J., and Kawata, Y. (1999) Unfolding and refolding of Escherichia coli chaperonin GroES is expressed by a three-state model. *J. Mol. Biol. 291*, 703–713.

(44) Seale, J. W., Gorovits, B. M., Ybarra, J., and Horowitz, P. M. (1996) Reversible oligomerization and denaturation of the chaperonin GroES. *Biochemistry 35*, 4079–4083.

(45) Bascos, N., Guidry, J., and Wittung-Stafshede, P. (2004) Monomer topology defines folding speed of heptamer. *Protein Sci. 13*, 1317–1321.

(46) Steede, N., Guidry, J., and Landry, S. (2000) Preparation of recombinant human cpn10. *Methods Mol. Biol. 140*, 145–151.

(47) Landry, S. J., Steede, N. K., and Maskos, K. (1997) Temperature dependence of backbone dynamics in loops of human mitochondrial heat shock protein 10. *Biochemistry 36*, 10975–10986.

(48) Ramsay, G., and Eftink, M. (1994) Analysis of multidimensional spectroscopic data to monitor unfolding of proteins. *Methods Enzymol. 240*, 615–645.

(49) Greenfield, N. (2006) Using circular dichroism collected as a function of temperature to determine the thermodynamics of protein unfolding and binding interactions. *Nature Protocols 1*, 2527–2535.

(50) Schellman, J. A. (1987) Selective binding and solvent denaturation. *Biopolymers 26*, 549–559.

(51) Hall, D., and Minton, A. P. (2003) Macromolecular crowding: qualitative and semiquantitative successes, quantitative challenges. *Biochim. Biophys. Acta 1649*, 127–139.

(52) Record, M. T., Jr., Courtenay, E. S., Cayley, S., and Guttman, H. J. (1998) Biophysical compensation mechanisms buffering E. coli protein-nucleic acid interactions against changing environments. *Trends Biochem. Sci. 23*, 190–194.

(53) Cayley, S., Lewis, B. A., Guttman, H. J., and Record, M. T. (1991) Characterization of the cytoplasm of Escherichia coli K-12 as a function of external osmolarity: Implications for protein-DNA interactions in vivo. *J. Mol. Biol. 222*, 281–300.

(54) Luke, K., Apiyo, D., and Wittung-Stafshede, P. (2005) Dissecting homo-heptamer thermodynamics by isothermal titration calorimetry: entropy-driven assembly of co-chaperonin protein 10. *Biophys. J. 89*, 3332–3336.

(55) Luke, K., Perham, M., and Wittung-Stafshede, P. (2006) Kinetic folding and assembly mechanisms differ for two homologous heptamers. *J. Mol. Biol. 363*, 729–742.

(56) Luke, K., and Wittung-Stafshede, P. (2006) Folding and assembly pathways of co-chaperonin proteins 10: Origin of bacterial thermostability. *Arch. Biochem. Biophys. 456*, 8–18.

(57) Perham, M., Chen, M., Ma, J., and Wittung-Stafshede, P. (2005) Unfolding of heptameric co-chaperonin protein follows "fly casting" mechanism: observation of transient nonnative heptamer. *J. Am. Chem. Soc. 127*, 16402–16403.

(58) Bohrer, M. P., GD, and Carroll, P. J. (1984) Hindered diffusion of dextran and Ficoll in microporous membranes. *Macromolecules 17*, 1170–1173.

(59) Davidson, M. D., and W. (1988) Hindered diffusion of water-soluble macromolecules in membranes. *Macromolecules 21*, 3474–3481.

(60) Ohlson, M., Sorensson, J., Lindstrom, K., Blom, A. M., Fries, E., and Haraldsson, B. (2001) Effects of filtration rate on the glomerular barrier and clearance of four differently shaped molecules. *Am. J. Physiol. Renal Physiol. 281*, F103–113.

(61) Oliver, J. D., 3rd, Anderson, S., Troy, J. L., Brenner, B. M., and Deen, W. H. (1992) Determination of glomerular size-selectivity in the normal rat with Ficoll. *J. Am. Soc. Nephrol. 3*, 214–228.

(62) Lavrenko, P. N., Mikriukova, O. I., and Okatova, O. V. (1987) On the separation ability of various Ficoll gradient solutions in zonal centrifugation. *Anal. Biochem. 166*, 287–297.

(63) Wilkins, D. K., Grimshaw, S. B., Receveur, V., Dobson, C. M., Jones, J. A., and Smith, L. J. (1999) Hydrodynamic radii of native and denatured proteins measured by pulse field gradient NMR techniques. *Biochemistry 38*, 16424–16431.

(64) Wallgren, M., Aden, J., Pylypenko, O., Mikaelsson, T., Johansson, L. B., Rak, A., and Wolf-Watz, M. (2008) Extreme temperature tolerance of a hyperthermophilic protein coupled to residual structure in the unfolded state. *J. Mol. Biol. 379*, 845–858.

(65) Galan, A., Sot, B., Llorca, O., Carrascosa, J. L., Valpuesta, J. M., and Muga, A. (2001) Excluded volume effects on the refolding and assembly of an oligomeric protein. GroEL, a case study. *J. Biol. Chem. 276*, 957–964.

(66) Minton, A. P. (2000) Effect of a concentrated "inert" macromolecular cosolute on the stability of a globular protein with respect to denaturation by heat and by chaotropes: a statistical-thermodynamic model. *Biophys. J. 78*, 101–109.

(67) Christiansen, A., Wang, Q., Samiotakis, A., Cheung, M. S., and Wittung-Stafshede, P. (2010) Factors defining effects of macromolecular crowding on protein stability: an in vitro/in silico case study using cytochrome c. *Biochemistry 49*, 6519–6530.

(68) Tellam, R. L., Sculley, M. J., Nichol, L. W., and Wills, P. R. (1983) The influence of poly(ethylene glycol) 6000 on the properties of skeletal-muscle actin. *Biochem. J. 213*, 651–659.

(69) Harding, S. E., Horton, J. C., Jones, S., Thornton, J. M., and Winzor, D. J. (1999) COVOL: an interactive program for evaluating second virial coefficients from the triaxial shape or dimensions of rigid macromolecules. *Biophys. J. 76*, 2432–2438.

(70) Fissell, W. H., Hofmann, C. L., Smith, R., and Chen, M. H. (2010) Size and conformation of Ficoll as determined by size-exclusion chromatography followed by multiangle light scattering. *Am. J. Physiol. Renal Physiol. 298*, F205–F208.

(71) Fodeke, A. A., and Minton, A. P. (2010) Quantitative characterization of polymer-polymer, protein-protein, and polymer-protein interaction via tracer sedimentation equilibrium. *J. Phys. Chem. B 114*, 10876–10880.

(72) Guven, O., and Eltan, E. (2003) Molecular association in aqueous solutions of high molecular weight poly(N-vinyl-2-pyrrolidone). *Makromol. Chem. 182*, 3129–3134.

(73) Okamoto, D. N., Oliveira, L. C., Kondo, M. Y., Cezari, M. H., Szeltner, Z., Juhasz, T., Juliano, M. A., Polgar, L., Juliano, L., and Gouvea, I. E. (2010) Increase of SARS-CoV 3CL peptidase activity due to macromolecular crowding effects in the milieu composition. *Biol. Chem. 391*, 1461–1468.

(74) Phillip, Y., Sherman, E., Haran, G., and Schreiber, G. (2009) Common crowding agents have only a small effect on protein-protein interactions. *Biophys. J. 97*, 875–885.

(75) Wilf, J., and Minton, A. P. (1981) Evidence for protein self-association induced by excluded volume. Myoglobin in the presence of globular proteins. *Biochim. Biophys. Acta 670*, 316–322.

(76) Kim, Y. C., Best, R. B., and Mittal, J. (2010) Macromolecular crowding effects on protein-protein binding affinity and specificity. *J. Chem. Phys. 133*, 205101.

(77) Snoussi, K., and Halle, B. (2005) Protein self-association induced by macromolecular crowding: a quantitative analysis by magnetic relaxation dispersion. *Biophys. J. 88*, 2855–2866.

(78) McGuffee, S. R., and Elcock, A. H. (2010) Diffusion, crowding & protein stability in a dynamic molecular model of the bacterial cytoplasm. *PLoS Comput. Biol. 6*, e1000694.

(79) Rivas, G., Fernandez, J. A., and Minton, A. P. (2001) Direct observation of the enhancement of noncooperative protein self-assembly by macromolecular crowding: indefinite linear self-association of bacterial cell division protein FtsZ. *Proc. Natl. Acad. Sci. U.S.A. 98*, 3150–3155.

(80) del Alamo, M., Rivas, G., and Mateu, M. G. (2005) Effect of macromolecular crowding agents on human immunodeficiency virus type 1 capsid protein assembly in vitro. *J. Virol. 79*, 14271–14281.

(81) Hong, J., and Gierasch, L. M. (2010) Macromolecular crowding remodels the energy landscape of a protein by favoring a more compact unfolded state. *J. Am. Chem. Soc. 132*, 10445–10452.

(82) Ando, T., and Skolnick, J. (2010) Crowding and hydrodynamic interactions likely dominate in vivo macromolecular motion. *Proc. Natl. Acad. Sci. U.S.A. 107*, 18457–18462.